

Equilibrium conformation of dimethylaminodichlorophosphine molecule: the use of the results of quantum-chemical calculations and spectroscopic measurements in the analysis of gas-phase electron diffraction data

L. S. Khaikin,^a O. E. Grikina,^a S. S. Kramarenko,^a E. A. Zhilinskaya,^b and B. I. Zhilinskii^b

^aDepartment of Chemistry, M. V. Lomonosov Moscow State University, Leninskie Gory, 119899 Moscow, Russian Federation.

Fax: +7 (095) 932 8846

^bLittoral University,
F-59140 Dunkirk, France.

Fax: (33) 28 65 8239

Geometric parameters and force fields of two stable isomers of dimethylaminodichlorophosphine molecule, a *gauche*-conformer with C_1 symmetry (**A**) and *anti*-conformer with C_s symmetry (**D**), resulting from internal rotation about the P–N bond, were calculated in the RHF/6-31G* approximation. Using the scaled quantum-chemical force field for the most stable conformer **A**, the first reliable interpretation of the vibrational spectra of the light and perdeuterated isotopomers of dimethylaminodichlorophosphine was obtained. The root-mean-square vibrational amplitudes, harmonic and anharmonic vibrational corrections, and centrifugal distortion corrections were also calculated. Structural analysis of electron diffraction data was performed with consideration of nonlinear kinematic effects at the first-order level of perturbation theory. The experimental values of the equilibrium geometric parameters were estimated. The results obtained suggest a nonplanar equilibrium configuration of the amino group in the dimethylaminodichlorophosphine molecule.

Key words: dimethylaminodichlorophosphine; gas-phase electron diffraction; nonempirical calculations; molecular structure; force field, scaling, normal coordinate analysis.

Aminophosphines represent an important and interesting class of compounds. However, no unambiguous interpretation of the results of structural and spectral studies is available so far even for the simplest aminophosphines. This also concerns dimethylaminodichlorophosphine (**1**), which was studied by various diffraction^{1–3} and spectroscopic^{4–12} methods. The molecule of this compound is symmetrically substituted at the N and P atoms (Fig. 1).

Conformational transitions in the aminophosphine molecules can occur due to internal rotation about the P–N bond and to a pyramidal inversion at the N and P atoms with the barriers estimated at ~40 kcal mol^{–1} for P and at only 1–2 kcal mol^{–1} for N.¹³ Therefore, only conformers with the "pyramidal" P atom and either "pyramidal" or "planar" N atom (**A**–**H**, see Fig. 1) can exist at not too high temperatures.

Most of the experimental data^{2–7} suggest that a *gauche*-conformation is the preferred ground-state conformation of molecule **1**. It should be emphasized that the ¹H NMR spectra^{4–6} allow either a "planar" equilibrium configuration of the N atom (**F**, see Fig. 1) or a time-averaged planar geometry, which is due to fast

inversion at the N atom, with a nonplanar equilibrium configuration of the amino group (**A**, see Fig. 1). According to the results of quantum-chemical calculations,^{2,3,14} the *gauche*-conformer with C_1 symmetry and nonplanar bonding at the N atom (**A**, see Fig. 1) corresponds to a minimum of the total energy of isolated molecule **1**, whereas the *gauche*-conformer with C_s symmetry and planar amino fragment (**F**, see Fig. 1) corresponds to the transition state (TS) of inversion at N. The temperature dependence of the ¹H NMR spectra^{4–6} and the low barrier to inversion^{2,3} suggest the possibility for a large-amplitude wagging-inversion motion to occur in the amino group.

As was shown in an X-ray diffraction study,² the molecule **1** adopts a *gauche*-conformation with C_s symmetry and planar amino fragment in the crystalline phase at –130 °C. The results of a recent gas-phase electron diffraction study³ differ from those obtained earlier¹ but are in agreement with the molecular structure of **1** in the crystalline phase. However, this contradicts the results of quantum-chemical calculations.^{2,3,14} Previously,^{1,3} structural analysis was performed in the so-called thermal-average structure approximation ($r_a \equiv r_g(1)$ and $r_a \equiv r_{h0}$, respectively)^{15,16}; however, these structures are known to be strongly influenced by vibrational effects. Therefore, application of this ap-

* Université du Littoral, F-59140 Dunkerque, France,
Fax: (33) 28 65 8239.

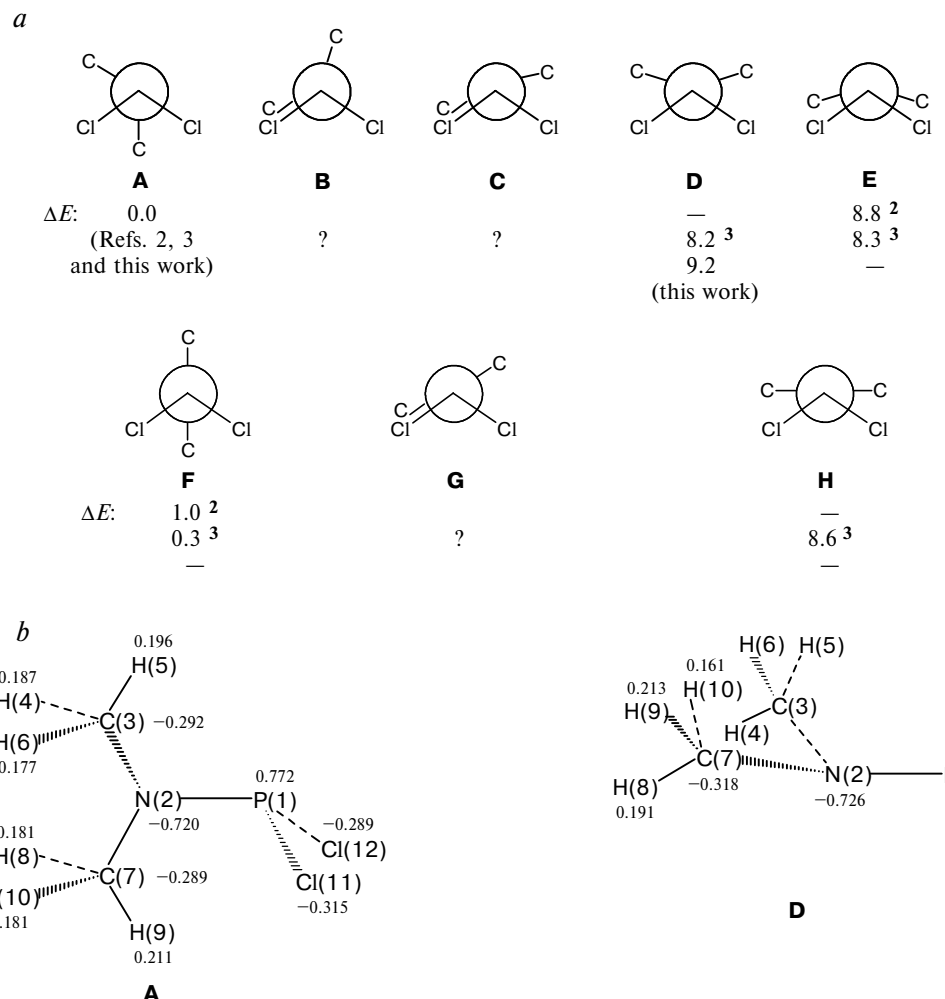


Fig. 1. Newman projections along the direction of the P–N bond for the conformations **A–H** of the Me_2NPCl_2 molecule, corresponding to different stationary points on the potential energy surface and the relative energies ($\Delta E/\text{kcal mol}^{-1}$) calculated in the MP2/6-311G*,² B3PW91/6-311+G*,³ and RHF/6-31G* (this work) approximations (a). Overall view of two equilibrium conformers of the Me_2NPCl_2 molecule, the *gauche*-conformer **A** with C_1 symmetry and the *anti*-conformer **D** with C_s symmetry. Shown are the atomic numbering scheme and the Mulliken atomic charges obtained from RHF/6-31G* calculations (b).

proximation to molecular systems with large-amplitude motions (e.g., molecule **1**) can lead to considerable uncertainties when estimating the equilibrium geometry.

In this connection, correct structural interpretation of the gas-phase electron diffraction data using adequate values of the moments of the probability density function of internuclear distances r_{ij} (the first absolute moments, or harmonic shrinkage corrections, δ_{ij}^{vib} , and the second central moments, which give the root-mean-square (RMS) vibrational amplitudes u_{ij}) becomes particularly topical. Recently,¹⁷⁻²⁰ we have shown that the use of the spectroscopic values of the parameters u_{ij} and δ_{ij}^{vib} calculated taking into account nonlinear kinematic effects at the first-order level of perturbation theory ($h1$)^{21,22} instead of the results obtained in the conventional small-amplitude harmonic vibration approximation ($h0$)^{15,16} allows one to circumvent many severe

difficulties when determining the molecular structure. The inclusion of nonlinear kinematic effects is of particular importance in the gas-phase electron diffraction studies of nonrigid structures to which molecule **1** tentatively belongs. Calculations of these parameters require a reliable force field.

Additionally, the lack of reliable force fields for compounds of the type $\text{Alk}_2\text{NPHal}_2$ precludes the resolution of the known contradictions^{10–12} in the assignment of the vibrational bands in the experimental spectra recorded by different authors and in some cases the rationalization of considerable differences between the spectra. Recently, high efficiency of the use of scaled quantum-chemical force field for this purpose was demonstrated.^{17–20} Solution of the inverse spectral problem by scaling of quantum-chemical force field provides an unambiguous assignment of the fundamental bands in the vibrational spectra.

In this work, geometric parameters of two stable isomers of molecule **1**, the *gauche*-conformer with C_1 symmetry and *anti*-conformer with C_s symmetry (**A** and **D**, respectively, see Fig. 1), resulting from internal rotation about the P—N bond, were optimized in the RHF/6-31G* approximation. The harmonic force fields, band intensities in the IR and Raman spectra, and depolarization degrees were also calculated. Using scaling of the quantum-chemical force field for the most stable conformer **A**, we first obtained a complete and unambiguous interpretation of the known^{10,11} IR spectra (in the range 33–4000 cm^{-1}) and Raman spectra (in the range 50–3000 cm^{-1}) of the light and perdeuterated isotopomers of compound **1**. A new assignment of most of the bands of skeletal deformation vibrations of the conformer **A** is proposed and the vibrational spectrum of the hypothetical *anti*-conformer **D** was calculated.

Based on the scaled quantum-chemical force field, we determined the RMS vibrational amplitudes, harmonic and anharmonic vibrational corrections, and centrifugal distortion corrections for internuclear distances in molecule **1**. In addition to the geometric parameters obtained from our quantum-chemical calculations, these vibrational amplitudes and corrections were used in the analysis of the gas-phase electron diffraction data¹ in the framework of the r_{h1} -structure,^{21,22} which is based on harmonic potentials, and for the evaluation of the equilibrium internuclear distances $r_{ij,e}$.

Experimental and calculation procedures

In this work, we used electron diffraction patterns of compound **1** in the gas phase, which were inadequately characterized earlier.¹ The sample of compound **1** synthesized following the known procedure²³ was characterized by a b.p. of 41–43 °C (14 mm Hg) and 73–75 °C (50 mm Hg) and a refractive index, n_{D}^{20} , of 1.5050 to 1.5055 (cf. b.p. 57–59 °C (24 mm Hg)⁶ and 150 °C (760 mm Hg)²³). Experiments were carried out on an "MGU" electron diffraction apparatus^{24,25} with an accelerating voltage of 60 keV and two nozzle–plate distances, 262.93 mm (LD) and 141.75 mm (SD), at ~325 K. At each distance, experiments were carried out using two different rotating sectors with the maximum radius of 30 mm (sector 1) and 45 mm (sector 2). The electron beam wavelength was determined using the diffraction patterns from the crystalline standard (ZnO) and the published data²⁶ on the interplanar distances in the crystal. Nine photoplates exposed to dimethylaminodichlorophosphine vapors were found to be suitable for structural analysis. The optical densities for these photoplates were measured on an MF-4 microphotometer.

The averaged total scattering intensity curves, $I^T(s)$, were calculated with an increment $\Delta s = 0.125 \text{ \AA}^{-1}$ for four sets of experimental data recorded with two rotating sectors at each nozzle–plate distance. Initially, the background lines, $I^B(s)$, were plotted using the results of quantum-chemical calculations of the molecular structure of **1**. Then, they were spline approximated and corrected in the course of the analysis. Smoothness of these curves characterizes the quality of the data used and the results of analysis. The experimental $I^T(s)$ curves and the final version of the $I^B(s)$ lines are presented in Fig. 2.

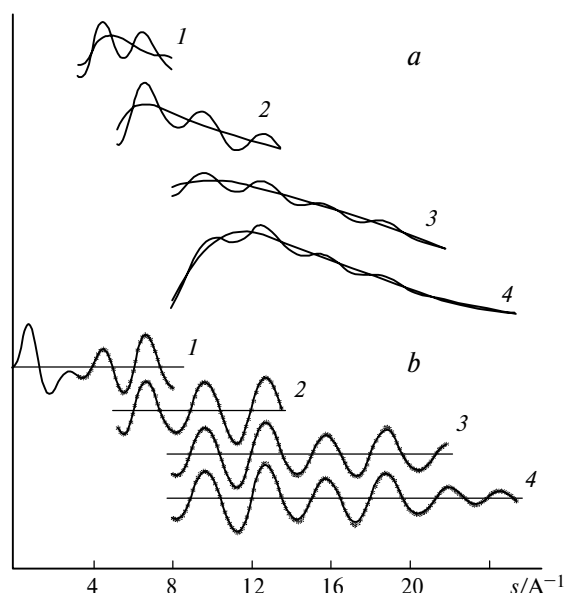


Fig. 2. The total scattering intensity curves, $I^T(s)$, and the background lines $I^B(s)$ for four sets of experimental data obtained with two different rotating sectors at nozzle–plate distances of ~263 mm (1, 2) and ~142 mm (3, 4) (a). Comparison of the experimental molecular scattering intensity curves $sM(s)$ (points) with the theoretical curves obtained for the version IIA of structural analysis (solid line) for the curves 1–4 (b).

Structural parameters were refined by the least squares processing of the experimental molecular scattering intensity curves $sM^{\text{exp}}(s)$ (see Fig. 2) with diagonal weight matrices. The theoretical molecular scattering intensities, $sM^{\text{theor}}(s)$, were calculated using complex scattering factors.²⁷ The anharmonicity parameters, $a_3(ij)$, for bonds were set equal to their values for diatomic molecules (2.009, 2.269, and 1.98 \AA^{-1} for the P—N, N—C, and C—H bonds, respectively. For P—Cl bonds, a value of 1.5 \AA^{-1} , which is close to that found for SiCl molecule, was used). For the distances between nonbonded atoms, these parameters were set to zero.²⁸ The experimental errors were estimated with inclusion of the standard deviations of the least squares method and scale errors.²⁹

The vibrational parameters $u_{ij,h1}$ and $\delta_{ij,h1}^{\text{vib}}$ were calculated at the first-order level of perturbation theory^{21,22} taking into account local centrifugal distortions due to intramolecular motions³⁰ (the problem of local centrifugal distortions was posed by Bartell³¹). Centrifugal distortions due to rotation of the entire molecule (δ_{ij}^{rot}) were calculated following the known procedure.³² The contributions of anharmonic terms of the Taylor expansion of the potential function $V(q)$ were estimated using the solution of the equations of motion for the molecular system at the first-order level of perturbation theory.³³ The diagonal cubic expansion terms corresponding to stretching vibrations were calculated as $h_{kkk} = -3f_{kk}a_3^{(k)}$, where $a_3^{(k)}$ is the cubic anharmonicity parameter in the diatomic approximation;²⁸ and all other cubic expansion terms were set to zero.

Analysis of vibrational spectra using the quantum-chemical force field was performed by fitting the calculated vibrational frequencies to the experimental data^{10,11} with refinement of the scale factor set.^{34,35} The matrix of the second derivatives of the total energy with respect to Cartesian atomic displacements, obtained from quantum-chemical calculations, was transformed to the complete system of independent local-symmetry internal

coordinates. The corresponding sets of the internal vibrational coordinates were discussed previously.³⁴ The scale factors, C_i , were introduced for i th groups of internal coordinates $\{m\}$ related by approximate local symmetry transformations. The quantum-chemical force constant matrix F_{mn}^{theor} was modified³⁵ using the diagonal matrix with the elements C_m according to the formula $F_{mn} = (C_m C_n)^{1/2} F_{mn}^{\text{theor}}$.

Structural analysis of the gas-phase electron diffraction data was performed using the KCED-25 program³⁶ adapted for IBM-compatible PC at the Electron Diffraction Team of the L. Eotvos Budapest University (Hungary) and modified at the M. V. Lomonosov Moscow State University (Russian Federation). Quantum-chemical calculations were carried out on an HP735 Work Station using the GAUSSIAN-92³⁷ program package at the Littoral University (Dunkerque, France). Spectroscopic calculations were carried out using the ANCO/SCAL/PERT^{38,39} and SHRINK^{21,22} (updated 2000 version) program packages.

Quantum-chemical estimates of changes in the energy and geometric parameters upon conformational transitions

Not only do the results of our RHF/6-31G* calculations represent a basis for normal coordinate analysis, but also indicate significant changes in the geometric parameters of molecule **1** due to internal rotation (Table 1). The *anti*-conformer **D** (its total energy is

9.2 kcal mol⁻¹ higher than that of the *gauche*-conformer **A**) is characterized by a substantial increase in "pyramidal" of the N atom (and, to a lesser extent, the P atom), by appreciable lengthening of the P—N and N—C bonds, and by shortening of the P—Cl bonds. On the other hand, the atomic charges (see Fig. 1) and, as a consequence, the dipole moments (see Table 1) of the two stable rotamers differ insignificantly. According to MP2 calculations,² the planar TS of nitrogen inversion at N (**F**) is also characterized by pronounced changes in geometric parameters as compared to the equilibrium *gauche*-conformer **A** (see Results and Discussion) while the height of the barrier to inversion equals 1 kcal mol⁻¹.

Interpretation of vibrational spectra using scaling of quantum-chemical force field

As far as we know, only one study¹² concerning the solution of the inverse spectral problem for three aminophosphines (compound **1**, its perdeuterated isotopomer, and Me_2NPF_2) using the conventional least-squares refinement of a common set of force constants is available in the literature. However, the approach used in the study¹² has some drawbacks. Calculations¹² were carried out based on the experimental band assignment

Table 1. Geometric parameters, dipole moments, and the total energies of the rotamers **A** and **D** of dimethylaminodichlorophosphine molecule obtained from RHF/6-31G* calculations

Parameter ^a	Rotamer		Parameter ^a	Rotamer	
	A	D		A	D
Bond		<i>r</i> /Å	Dihedral angle		τ /deg
P—N	1.6552		Cl(11)—P—N—C(3)	110.2	-165.0
N—C(3)	1.4591		Cl(12)—P—N—C(3)	-148.1	-62.7
N—C(7)	1.4555	}	Cl(11)—P—N—C(7)	-48.2	62.7
C(3)—H(4)	1.0840		Cl(12)—P—N—C(7)	53.5	165.0
C(7)—H(8)	1.0840		H(4)—C(3)—N—P	140.1	} ± 170.7
C(3)—H(5)	1.0818		H(8)—C(7)—N—P	-144.8	
C(7)—H(9)	1.0790		H(8)—C(7)—N—C(3)	56.3	} ± 55.2
C(3)—H(6)	1.0866		H(4)—C(3)—N—C(7)	-59.0	
C(7)—H(10)	1.0861		H(5)—C(3)—N—P	21.1	} ± 52.8
P—Cl(11)	2.0946		H(9)—C(7)—N—P	-25.6	
P—Cl(12)	2.0718		H(9)—C(7)—N—C(3)	175.4	} ± 173.1
Bond angle		β /deg	H(5)—C(3)—N—C(7)	-178.0	
N—P—Cl(11)	103.9		H(10)—C(7)—N—P	95.2	} ± 69.7
N—P—Cl(12)	101.8		H(6)—C(3)—N—P	-99.8	
Cl—P—Cl	98.3		H(6)—C(3)—N—C(7)	61.1	} ± 64.4
P—N—C(3)	117.1		H(10)—C(7)—N—C(3)	-63.8	
P—N—C(7)	125.5		Cl(11)—P—N/Cl(12)—P—N (γ)	78.3	77.7
C—N—C	114.2		C(3)—N—P/C(7)—N—P (δ)	21.6	47.7
N—C(3)—H(4)	109.3		ϕ ^b	81.9	0.0
N—C(7)—H(8)	109.2		Dipole moment		μ /D
N—C(3)—H(5)	110.5			3.83	3.70
N—C(7)—H(9)	110.7		Total energy		$-(E + 1393.0)/\text{au}$
N—C(3)—H(6)	111.5			0.398797	0.384110
N—C(7)—H(10)	111.0				

^a The atomic numbering scheme is shown in Fig. 1.

^b The angle between the bisecting planes of the dihedral angles γ and δ .

Table 2. Nonredundant set of local-symmetry internal coordinates for dimethylaminodichlorophosphine molecule and the scale factors for the quantum-chemical force field of conformer **A** calculated in the RHF/6-31G* approximation

Number	Notation ^a	Coordinate	Scale factor
		Instance of coordinate definition	
1, 2	NC str	N(2)C(3) str	0.8120
3, 4	PCl str	P(1)Cl(11) str	0.8144
5	PN str	P(1)N(2) str	0.9016
6	PN rock	(P(1)N(2)C(3) bend – P(1)N(2)C(7) bend)/ $\sqrt{2}$	0.8022
7	PN wag	P(1)N(2)/C(3)N(2)C(7) out-of-plane bond deviation	0.8998
8	CNC def	(2 C(3)N(2)C(7) bend – P(1)N(2)C(3) bend – P(1)N(2)C(7) bend)/ $\sqrt{6}$	0.8114
9, 10	NPCl bend	N(2)P(1)Cl(11) bend	0.7951
11	CIPCl bend	Cl(11)P(1)Cl(12) bend	0.8069
12, 13	Me s.str	(C(3)H(4) str + C(3)H(5) str + C(3)H(6) str)/ $\sqrt{3}$	0.7977
14, 15	Me str A	(2 C(3)H(4) str – C(3)H(5) str – C(3)H(6) str)/ $\sqrt{6}$	
16, 17	Me str B	(C(3)H(5) str – C(3)H(6) str)/ $\sqrt{2}$	
18, 19	Me s.def	(H(5)C(3)H(6) bend + H(4)C(3)H(6) bend + H(4)C(3)H(5) bend – N(2)C(3)H(4) bend – N(2)C(3)H(5) bend – N(2)C(3)H(6) bend)/ $\sqrt{6}$	
20, 21	Me def A	(2 H(5)C(3)H(6) bend – H(4)C(3)H(6) bend – H(4)C(3)H(5) bend)/ $\sqrt{6}$	0.7935
22, 23	Me def B	(H(4)C(3)H(6) bend – H(4)C(3)H(5) bend)/ $\sqrt{2}$	
24, 25	Me rock \parallel	(2 N(2)C(3)H(4) bend – N(2)C(3)H(5) bend – N(2)C(3)H(6) bend)/ $\sqrt{6}$	
26, 27	Me rock \perp	(N(2)C(3)H(5) bend – N(2)C(3)H(6) bend)/ $\sqrt{2}$	0.7669
28, 29	Me tors	(H ₃ C(3)–N(2)(P(1),C(7)) tors	
30	PN tors	(Cl ₂)P(1)–N(2)(C ₂) tors	

^a Notations of vibrations: str is stretching; bend is bending for the bond angle; def is local-symmetry deformation vibration for methyl or amino group; rock is rocking (\parallel and \perp denote parallel and normal to the local symmetry plane containing a given Me group); wag is wagging; tors is torsional (defined as the sum of the motions in the tetraatomic fragments); and s is symmetric vibration. Quasi-degenerate vibrations are labeled by A and B. The atomic numbering scheme is shown in Fig. 1.

reported in the first out of two alternative studies of the spectra of Me₂NPF₂.^{40,41} Additionally, torsional vibrations of Me groups were not considered, which led to considerable uncertainties in the band assignment in the low-frequency region (this spectral region is of prime importance when calculating vibrational parameters for the analysis of gas-phase electron diffraction data).

Spectral analysis performed in this work is based on the scaling of the quantum-chemical force field of the stable conformer **A** of molecule **1** over the vibrational frequencies of two isotopomers.^{10,11} The refined scale factors corresponding to different internal coordinates vary between 0.77 and 0.90 (Table 2) and their values are in good agreement with those we found earlier^{42–44} for other classes of compounds containing the same structural fragments. Transferability of the scale factors obtained allows one to reliably predict the values of force constants and, hence, the vibrational spectrum of the hypothetical *anti*-conformer **D** of molecule **1**.

The scaled quantum-chemical force fields of both stable rotamers of molecule **1** are listed in Table 3. They contain rather large force constants of interactions between internal coordinates corresponding mainly to vibrations of the heavy-atom molecular skeleton. On going from one conformer to the other the diagonal force constants of the skeletal (both stretching and deformation) vibrations change antiparallel to the changes in the corresponding geometric parameters (*cf.* the data listed in Tables 1 and 3). The force constants for the vibra-

tions of the Me groups of both conformers have very close values and can be considered transferable.

Compared to the force field calculated in this work for *gauche*-conformer **A**, the empirical force field of molecule **1** (see Ref. 12) is characterized by a much smaller number of nonzero interaction constants. Due to the differences between the internal coordinates used in both studies, we cannot compare all the force constants. Nevertheless, some substantial differences in magnitude of the force constants should be pointed out. For instance, the empirical constant of torsional vibration about the P–N bond (0.31 mdyn Å¹²) is overestimated while the that of the wagging-inversion vibration of amino group (PN wag, 0.11 mdyn Å¹²) is underestimated by a factor of 1.5. The empirical constants of the interactions NC str/NC str (0.32 mdyn Å^{−1}),¹² NC str/CNC def (0.17 mdyn),¹² and NPCl bend/NPCl bend (0.46 mdyn Å¹²) are much larger, while those of the interactions NC str/PN str (0.06 mdyn Å^{−1})¹² and CIPN bend/CIPCl bend (0.11 mdyn Å¹²)¹² are much smaller than the corresponding parameters of scaled quantum-chemical force field (see Table 3).

The mean deviation of the experimental frequencies of the light and perdeuterated isotopomers^{10,11} from the theoretical estimates of the frequencies of the *gauche*-conformer **A** lie between 6 and 8 cm^{−1} (from 1.4 to 1.9%). Our interpretation of the spectra (Table 4) is also confirmed by good correspondence between the calculated intensities and depolarization degrees and the

Table 3. Scaled force constants (in internal coordinates) for two stable rotamers, **A** and **D**, of dimethylaminodichlorophosphine molecule^{a,b}

Force constant	Isomer		Force constant	Isomer	
	A	D		A	D
NC(3) str, NC(7) str*	4.71, 4.73*	4.58	CNC def	0.85	1.14
/PN str	0.25, 0.24*	0.25	/NPCl(11) bend	-0.02	} -0.19
/PN rock	0.25, -0.24*	±0.26	/NPCl(12) bend	-0.12	
/PN wag	-0.07, -0.05*	-0.15	NPCl(11) bend, NPCl(12) bend*	1.20, 1.41*	1.42
/CNC def	0.07, 0.09*	0.17	/NPCl bend	0.26	0.10
/Me s.str ^c	0.25, 0.23*	0.23	/CIPCl bend	0.21, 0.24*	0.10
/Me s.def ^c	-0.46	-0.45	/PN tors	0.04, 0.02*	±0.14
PCI(11) str, PCI(12) str*	1.94, 2.19*	2.14	CIPCl bend	1.26	1.17
/PCI str	0.23	0.22	Me(C3) s.str, Me(C7) s.str*	4.76, 4.80*	4.78
/PN str	0.31, 0.27*	0.30	/Me str B ^c	0.07, -0.10*	0.16
/NPCl bend ^c	0.17, 0.20*	0.17	/Me s.def ^c	0.10	0.11
/CIPCl bend	0.19, 0.20*	0.11	Me(C3) str A, Me(C7) str A*	4.62, 4.65*	4.66
PN str	5.05	4.07	/Me str B ^c	-0.06, 0.09*	-0.13
/PN wag	-0.16	-0.20	/Me def A ^c	-0.13	-0.13
/CNC def	-0.26	-0.28	Me(C3) str B, Me(C7) str B*	4.63, 4.69*	4.62
/NPCl(11) bend	0.18	} 0.33	/Me def B ^c	-0.13, -0.13*	-0.13
/NPCl(12) bend	0.32		Me s.def	0.61	0.60
PN rock	0.80	0.86	Me(C3) def A, Me(C7) def A*	0.55, 0.55*	0.57
/NPCl(11) bend	0.02	} ±0.12	Me(C3) def B, Me(C7) def B*	0.55, 0.55*	0.55
/NPCl(12) bend	-0.06		Me rock 	0.76	0.77
/PN tors	-0.08	-0.40	Me rock⊥	0.75	0.74
PN wag	0.16	0.26	Me(C3) tors, Me(C7) tors*	0.07, 0.05*	0.07
/CNC def	-0.05	-0.19	PN tors	0.21	0.25

^a For notations of vibrations, see note to Table 2. The atomic numbering scheme is shown in Fig. 1.

^b For each coordinate, the diagonal force constant indicated in boldface print (one out of the two contiguous coordinates corresponding to different structural fragments is asterisked) is followed by the force constants of interaction between this and other coordinates (slashed). The force constants of stretching vibrations and interactions between them are given in mdyn Å⁻¹, those of interactions between stretching and deformation (including torsional) vibrations are given in mdyn, and those of all types of deformation vibrations and interactions between them are given in mdyn Å. Off-diagonal force constants whose moduli do not exceed 0.1 are not listed.

^c The interaction with the coordinate corresponding to the adjacent structural fragment.

experimental data. Compared to the known band assignment, we propose a nearly completely new assignment of the bands observed in the frequency range below 400 cm⁻¹ and corresponding to the skeletal deformation vibrations and torsional vibrations for both isotopomers. The normal modes in the frequency range below 1300 cm⁻¹ are characterized by large contributions of the skeletal vibrations and significant mixing.

Among low-frequency normal vibrations, only the antiphase torsional motion of Me groups can be considered pure. In the spectra of both isotopomers, this vibration corresponds to the very weak bands at 155 and 120 cm⁻¹ (ν_{28} , see Table 4). According to our calculations, the largest contribution of the torsional vibration about the P—N bond corresponds to the lowest lying bands at 55 and 45 cm⁻¹ in the spectra of both isotopomers, which were not detected experimentally due to their very low intensities (ν_{30} , see Table 4).

Comparing the spectrum of the *anti*-conformer **D** of molecule **1** with that of the *gauche*-conformer **A**, one can see that the frequency shifts for some stretching vibrations are as large as 40 cm⁻¹.

Calculations of the RMS vibrational amplitudes, vibrational corrections, and centrifugal distortion corrections for internuclear distances

The harmonic vibrational corrections, $\delta_{ij,h1}^{\text{vib}}$, calculated in this work at the first-order level of perturbation theory are listed in Table 5. For bonds, they are completely determined by the contributions of local centrifugal distortions³⁰ that are due to deformation vibrations. These contributions, including those for the distances between nonbonded non-hydrogen atoms, are at most 0.003–0.004 Å at 298 K.

Peculiarities of the molecular structure of **1** manifest themselves as the influence of nonlinear kinematic effects on the RMS vibrational amplitudes u_{ij} for the distances between the nonbonded atoms of the PNC₂ fragment and the C...Cl distances. An increase in the parameters $u_{ij,h1}$ compared to $u_{ij,h0}$ for the fragment PNC₂ can be rationalized only by an increase in the amplitude of the wagging-inversion motion in the amino group. In the case of the RMS vibrational amplitudes for the C...Cl distances this effect is combined with the

Table 4. Band assignment in the experimental IR and Raman spectra of isomer A of dimethylaminodichlorophosphine molecule (performed using scaling of quantum-chemical force field)^a

Vibration		Calculations						Experiment ^{10,11} , ν/cm^{-1} ^d				
No.	Mode	$(\text{CH}_3)_2\text{NPCl}_2$			$(\text{CD}_3)_2\text{NPCl}_2$			$(\text{CH}_3)_2\text{NPCl}_2$		$(\text{CD}_3)_2\text{NPCl}_2$		
		ν/cm^{-1}	PED (%)	IR, I^b	Raman, I^c	Depol.	ν/cm^{-1}	PED (%)	IR ^e	Raman ^f	IR ^e	Raman ^f
1	Me(C7) str B	2983.4	64	10.1	34.5	0.68	2212.0	65	2985 w	2981 w dp	2220 vw	2224 m dp
	Me(C7) str A		27					31				
2	Me(C3) str B	2952.8	57	21.0	55.1	0.74	2191.1	55	2940 w	2949 m p?	2210 w	2209 m dp
	Me(C3) str A		40					43				
3	Me(C7) str A	2921.5	72	40.5	85.0	0.61	2167.4	68	2940 w	2922 w	—	—
	Me(C7) str B		23					31				
4	Me(C3) str A	2917.6	59	30.6	78.5	0.59	2164.0	56	2900 m ^h	2909 w p	—	—
	Me(C3) str B		33					42				
5	Me(C7) s.str	2867.4	78	61.1	157.3	0.04	2060.9	85	2848 w ^h	2850 m p	2072 m	2067 s p
6	Me(C3) s.str	2858.6	80	44.0	51.7	0.07	2052.7	86	2848 w ^h	2850 m p	2065 m	2067 s p
7	Me def B synph	1484.2	57	6.5	29.3	0.70	1069.4	60	1484 m ^h	1480 w dp	—	1065 vw
	Me def A synph		29					38				
8	Me def B antiph	1468.5	68	13.3	2.7	0.64	1061.3	65	1474 m ^f	1480 w dp	—	1065 vw
	Me def A antiph		26					33				
9	Me def A synph	1462.0	64	15.8	1.5	0.73	1054.9	61	1459 m ^h	—	1055 m	1055 vw
	Me def B synph		29					36				
10	Me def A antiph	1450.0	66	4.4	15.3	0.73	1046.5	63	1449 m ^h	—	1045 m	1045 vw
	Me def B antiph		27					34				
11	Me s.def synph	1439.0	97	1.9	16.0	0.75	1107.7	91	1438 m ^h	1438 m dp	—	1110 vw
12	Me s.def antiph	1409.7	100	0.8	8.4	0.74	1039.5	81	1408 w ^f	1411 w dp	1035 w ^e	—
13	Me rock \perp synph	1293.5	31	81.0	0.2	0.57	1211.9	15	1282 w	1290 vw p	1201 s	1205 vw
	PN str		17					31	(1287 s) ^h			
	NC ₂ s.str		14					33				
14	NC ₂ as.str	1178.8	70	78.4	0.4	0.67	1168.2	73	1173 m ^h	1176 vw	1172 m	—
15	Me rock \parallel synph	1120.5	60	9.1	1.3	0.58	888.2	60	1120 w	—	906 w ^e	—
	Me rock \perp synph		32					34				
16	Me rock \parallel antiph	1075.1	57	2.7	3.8	0.75	817.1	45	1058 m ^h	1067 w dp	835 m	832 w p
	Me rock \perp antiph		37					22				
17	Me rock \perp antiph	1043.6	46	21.4	7.4	0.74	805.4	73	1028 m ^h	—	795 w	—
	Me rock \parallel antiph		26					16				
	NC ₂ as.str		24					7				
18	NC ₂ s.str	975.1	42	206.4	6.4	0.74	813.9	11	988 s	980 w dp	828 m	—
	PN str		24					6				
	Me rock \perp synph		23					33				
	Me rock \parallel synph		12					44				
19	PN str	677.7	52	49.9	8.7	0.14	630.1	48	675 w	690 s p	640 m	649 s p
	NC ₂ s.str		45					42				
20	PCl(12) str	512.2	51	88.1	14.7	0.12	506.0	56	505 s	515 m p	508 s	509 s p
	PN rock		19					15				
	NPCL(11) wag		16					15				
21	PCl(11).str	457.4	57	187.4	12.9	0.65	454.7	64	457 m	430 m dp	455 s	427 m dp
	PCl(12) str		20					17				
	NPCL(11) bend		14					12				
22	CNC def	391.6	50	26.6	6.1	0.22	357.5	23	396 m	394 m p	368 w	363 vs p
	PCl ₂ s.str		18					25			(358 m) ^h	
	PCl ₂ wag		12					22				
	PN rock		9					17				
23	CNC def	336.8	33	6.9	6.8	0.12	302.6	53	341 m	340 m p	308 m ^h	310 s p
	PN rock		26					15				
	PCl ₂ s.str		26					13				
24	PN wag	313.8	38	1.8	4.0	0.75	292.3	31	292 vw ^h	304 w	265 w ^h	287 w
	PCl ₂ twist		31					40				
	PCl ₂ as.str		16					14				
25	CIPCl bend	212.1	56	2.3	2.8	0.56	203.6	70	221 m ^h	216 m p	213 m ^h	210 m p
	PN rock		25					23				

(to be continued)

Table 4 (continued)

Vibration		Calculations						Experiment ^{10,11} , v/cm ⁻¹ ^d				
No.	Mode	(CH ₃) ₂ NPCl ₂			(CD ₃) ₂ NPCl ₂			(CH ₃) ₂ NPCl ₂		(CD ₃) ₂ NPCl ₂		
		v /cm ⁻¹	PED (%)	IR, I ^b	Raman, I ^c	Depol.	v /cm ⁻¹	PED (%)	IR ^e	Raman ^f	IR ^e	Raman ^f
26	Me(C3) tors	198.9	59	0.4	0.9	0.75	158.3	40	193 w	191 m dp	140 w ^h	142 w ^h
	PCl ₂ twist		29					28				
27	PCl ₂ wag	182.5	48	3.7	3.1	0.75	177.0	54	193 w	191 m dp	186 m ^h	190 m dp
	CIPCl bend		34					20				
	PN rock		11					17				
28	Me tors antiph	160.1	90	0.8	0.6	0.72	116.6	91	155 vw ^h	—	—	119 w ^e
29	PN wag	109.6	31	3.0	1.6	0.68	93.1	17	—	124 w	102 vw ^h	—
	PN tors		24					31				
	PCl ₂ twist		23					14				
	Me(C7) tors		16					32				
30	PN tors	54.4	68	0.7	0.3	0.69	47.3	62	—	—	—	—
	PN wag		25					24				
	Me tors synph		8					15				

^a See note to Table 2; PED is the potential energy distribution; synph and antiph denote the in-phase and antiphase vibration, respectively.

^b Intensity, I/km mol⁻¹.

^c I/A⁴ amu⁻¹.

^d Notations: m, s, vs, w, and vw is medium, strong, very strong, weak, and very weak band intensity, respectively; p and dp denote polarized and depolarized Raman lines, respectively.

^{e,f,h} Taken from the gas-phase, liquid-phase, and solid-phase spectra, respectively.

contribution of internal rotation about the P—N bond. Relatively weak influence of nonlinear kinematic effects on the RMS vibrational amplitudes obtained from spectroscopic calculations (see Table 5) represents an indi-

rect proof^{17–20} that the small-amplitude harmonic vibration approximation is sufficient to account for these effects when performing structural analysis of gas-phase electron diffraction data for molecule **1**.

Table 5. Root-mean-square amplitudes (u_{ij}) and vibrational corrections (δ_{ij}^{vib}) calculated in the conventional small-amplitude harmonic vibration approximation ($h0$) and at the first-order level of perturbation theory (harmonic $h1$, anharmonic $anh1$), and centrifugal distortion corrections (δ_{ij}^{rot}) for the internuclear distances in the conformer **A** of Me₂NPCl₂ molecule (in Å)

Distance ^a	$r_e/\text{\AA}^b$	$T = 0 \text{ K}$				$T = 298 \text{ K}$						
		u_{h0}	$\delta_{h0}^{\text{vib}} \equiv K_0$	u_{h1}	δ_{h1}^{vib}	$\delta_{anh1}^{\text{vib}}$	u_{h0}	$\delta_{h0}^{\text{vib}} \equiv K_T$	u_{h1}	δ_{h1}^{vib}	δ^{rot}	$\delta_{anh1}^{\text{vib}}$
P—N	1.6552	0.0432	0.0021	0.0432	0.0008	0.0018	0.0451	0.0036	0.0451	0.0009	0.0001	0.0037
N—C(3)	1.4591	0.0491	0.0084	0.0491	0.0004	0.0047	0.0497	0.0479	0.0497	0.0010	0.0002	0.0052
N—C(7)	1.4555	0.0490	0.0046	0.0490	0.0007	0.0034	0.0496	0.0113	0.0496	0.0012	0.0001	0.0025
C—H(av.)	1.0836	0.0789	0.0306	0.0789	0.0041	0.0161	0.0789	0.0848	0.0789	0.0043	0.0000	0.0167
P—Cl(11)	2.0946	0.0485	0.0017	0.0485	0.0003	0.0049	0.0559	0.0061	0.0559	0.0011	0.0005	0.0067
P—Cl(12)	2.0718	0.0470	0.0016	0.0470	0.0003	0.0046	0.0538	0.0046	0.0538	0.0009	0.0007	0.0060
P...C(3)	2.6585	0.0598	0.0033	0.0600	-0.0032	0.0029	0.0734	0.0191	0.0752	-0.0131	0.0007	0.0032
P...C(7)	2.7670	0.0569	0.0019	0.0571	-0.0034	0.0062	0.0652	0.0058	0.0667	-0.0117	0.0007	0.0073
C...C	2.4471	0.0652	0.0061	0.0654	-0.0049	0.0070	0.0727	0.0351	0.0739	-0.0132	0.0003	0.0078
N...H(av.)	2.0966	0.1041	0.0204	0.1046	-0.0018	0.0133	0.1051	0.0724	0.1058	-0.0010	0.0001	0.0132
N...Cl(11)	2.9655	0.0665	0.0014	0.0665	-0.0001	0.0035	0.0900	0.0055	0.0900	-0.0004	0.0010	0.0054
N...Cl(12)	2.9036	0.0628	0.0015	0.0628	-0.0006	0.0016	0.0838	0.0052	0.0838	-0.0011	0.0013	0.0031
Cl...Cl	3.1515	0.0637	0.0010	0.0637	0.0000	0.0041	0.0928	0.0049	0.0929	-0.0004	0.0014	0.0055
C(3)...Cl(11)	3.9516	0.0990	0.0011	0.0994	-0.0073	0.0055	0.2295	0.0047	0.2317	-0.0337	0.0038	0.0069
C(3)...Cl(12)	4.2181	0.0705	0.0012	0.0709	-0.0072	0.0062	0.1107	0.0067	0.1147	-0.0363	0.0001	0.0076
C(7)...Cl(11)	3.3694	0.0947	0.0015	0.0950	-0.0026	0.0034	0.1673	0.0065	0.1687	-0.0112	0.0025	0.0041
C(7)...Cl(12)	3.3471	0.0855	0.0016	0.0858	-0.0029	0.0035	0.1404	0.0062	0.1428	-0.0157	0.0021	0.0041

^a The atomic numbering scheme is shown in Fig. 1. The abbreviation av. denotes the average value of the parameter.

^b Obtained from RHF/6-31G* calculations.

The anharmonic corrections $\delta_{ij,anh1}^{\text{vib}}$ listed in Table 5 were calculated for a total of $3N - 7$ degrees of freedom left after exclusion of the lowest lying torsional mode. We found that consideration of this mode leads to large errors and excluded it from the solution of the spectral problem based on the assumption that cubic anharmonicity corrections should be first of all determined by the contributions of relatively high-frequency breathing modes corresponding to a simultaneous in-phase stretch or contraction of all bonds.³³ Though the calculated corrections $\delta_{ij,anh1}^{\text{vib}}$ are relatively small, there is no point in using them directly for structural analysis, since the known procedure³³ overestimates the results of calculations by ~40%. They can be considered only as the upper bound of the error due to neglect of the contributions of cubic terms of the Taylor expansion of the potential function.

Structural analysis

To illustrate complexity of the solution of the inverse problem in the gas-phase electron diffraction study of molecule **1**, suffice it to say that, according to quantum-chemical calculations, the nonsymmetric *gauche*-conformer **A** is characterized by different values of geometric parameters belonging to the same type, *e.g.*, the P—Cl or N—C bond lengths (see Table 1). Moreover, most of the nonbonded distances between the skeleton atoms contribute to only one peak on the experimental radial distribution curve $f(r)$ (at $r \approx 3 \text{ \AA}$, Fig. 3). Practically, it is impossible to resolve such small splittings and the overlap of the contributions of particular geometric parameters without invoking the data obtained by other methods.

The results of quantum-chemical and spectroscopic calculations allowed us to analyze the gas-phase electron diffraction data for molecule **1** using a molecular model, which implies the existence of one conformer, namely, the most stable *gauche*-conformer **A**, without considering large-amplitude motions in the framework of the so-called dynamic model. As is known, quantum-chemical estimates of the bond angles, dihedral angles, and splittings of the C—H bond lengths in the Me groups are virtually independent of the procedure for inclusion of electron correlation and are in good agreement with the experimental data (see, *e.g.*, Refs. 17–20). In the model used in this work, these parameters were assumed to have fixed values we obtained from RHF/6-31G* calculations, while the difference between two N—C bond lengths was set to 0.005 Å according to the results of MP2/6-311G** calculations.²

Table 6 lists the results of optimization of the geometric parameters of molecule **1**, obtained using the RMS vibrational amplitudes and vibrational corrections for internuclear distances calculated in the conventional small-amplitude harmonic vibration approximation (version I, r_{α} -structure)^{15,16} and with consideration of non-

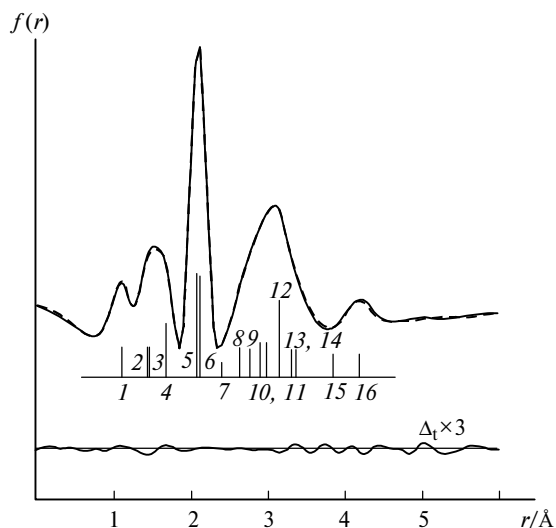


Fig. 3. Experimental (dashed line) and theoretical (solid line) radial distribution and the difference curve ($\Delta \times 3$) curves for version IIA of structural analysis of dimethylaminodichlorophosphine. Shown are the positions of the following most important internuclear distances: C—H (av.) (1); N—C(7) (2); N—C(3) (3); P—N (4); P—Cl(12) (5); P—Cl(11) (6); C...C (7); P...C(3) (8); P...C(7) (9); N...Cl(12) (10); N...Cl(11) (11); Cl...Cl (12); C(7)...Cl(11) (13); C(7)...Cl(12) (14); C(3)...Cl(11) (15), and C(3)...Cl(12) (16). The lengths of the vertical lines denote the relative contributions of corresponding distances. The damping constant was set to 0.0036 \AA^2 .

linear kinematic effects at the first-order level of perturbation theory (version II, two data sets, r_{h1} -structure).^{21,22,30} Table 7 lists the estimates of the parameters $r_{ij,a}^0$ and $r_{ij,h1}^0$ for the ground vibrational state, obtained after introducing partial anharmonic corrections calculated in the diatomic approximation¹⁶, $r_{ij,g} - r_{ij,g}^0 \equiv 1.5a_3(u_{ij}^2(T) - u_{ij}^2(0))$, and the corrections $\delta_{ij,h0}^{\text{vib}} = K_{ij}$ or $\delta_{ij,h1}^{\text{vib}}$ for $T = 0 \text{ K}$. Table 7 also lists the estimates of the parameters of the equilibrium r_e -structure, obtained after correcting the parameters of r_{h1} -structure for anharmonicity and centrifugal distortion using the $\delta_{ij,anh1}^{\text{vib}}$ and δ_{ij}^{rot} values, respectively (the validity of this procedure is based on the additivity of contributions in calculations at the first-order level of perturbation theory).

The convergence factors (R -factors) obtained for versions I and especially IIA of structural analysis (see Table 6) indicate good agreement between the theory and experiment when using the RMS vibrational amplitudes found from spectroscopic calculations. The found molecular scattering intensity parameters $r_{ij,a}$ depend only slightly on the type of approximation used for the calculations of vibrational characteristics for internuclear distances (except for the $r_{ij,a}$ parameters for the C—H and N—C bonds). The inclusion of the RMS vibrational amplitudes into the set of the parameters to be refined (see Table 6, version IIB) does not make the situation (*i.e.*, agreement with the experiment) better. Rather, it leads to a substantial increase in the least-squares pro-

Table 6. Results of analysis of gas-phase electron diffraction data for dimethylaminodichlorophosphine ($T = 325$ K) in the conventional small-amplitude harmonic vibration approximation (I) and with inclusion of nonlinear kinematic effects (II)

Parameter	I				IIA				IIB	
	r_a	$r_a - r_a$	$r_{\alpha} \equiv r_{h0}$	u_{h0}	r_a	$r_{h1} - r_a$	r_{h1}	u_{h1}	r_{h1}	u_{h1}
Bond length										
P—N	1.6699	-0.0026	1.667(4)	0.0455	1.6680	0.0003	1.668(4)	0.0455	1.668(4)	0.044(3) ^b
N—C(3)	1.4744	-0.0504	1.424(3)	0.0500	1.4530	0.0006	1.454(3)	0.0500	1.454(3)	0.048 ^b
N—C(7)	1.4295	-0.0104	1.419(3)	0.0498	1.4481	0.0005	1.449(3)	0.0498	1.449(3)	0.048 ^b
C(3)—H(4)	1.0888	-0.0823	1.007(4)	0.0790	1.0918	0.0014	1.093(3)	0.0790	1.093(3)	0.077 ^b
C(7)—H(8)	1.1047	-0.0981	1.007(4)	0.0790	1.0918	0.0014	1.093(3)	0.0790	1.093(3)	0.077 ^b
C(3)—H(5)	1.0552	-0.0508	1.004(3)	0.0786	1.0897	0.0014	1.091(3)	0.0786	1.091(3)	0.077 ^b
C(7)—H(9)	1.0974	-0.0959	1.002(4)	0.0781	1.0868	0.0014	1.088(3)	0.0782	1.088(3)	0.077 ^b
C(3)—H(6)	1.0957	-0.0866	1.009(4)	0.0794	1.0945	0.0013	1.096(3)	0.0794	1.096(3)	0.078 ^b
C(7)—H(10)	1.1076	-0.0990	1.009(4)	0.0793	1.0939	0.0014	1.095(3)	0.0794	1.095(3)	0.078 ^b
P—Cl(11)	2.1132	-0.0051	2.108(5)	0.0573	2.1103	0.0003	2.111(5)	0.0573	2.106(12)	0.0573
P—Cl(12)	2.0724	-0.0035	2.069(5)	0.0551	2.0739	0.0005	2.074(5)	0.0551	2.078(10)	0.0551
Distance ^a										
P...C(3)	2.6122	-0.0186	2.594(7)	0.0753	2.6191	0.0164	2.635(8)	0.0773	2.635(21)	0.081(29) ^c
P...C(7)	2.7605	-0.0047	2.756(7)	0.0666	2.7639	0.0144	2.778(7)	0.0683	2.775(8)	0.072 ^c
C...C	2.3920	-0.0360	2.356(10)	0.0741	2.3987	0.0163	2.415(10)	0.0755	2.406(16)	0.089(43)
N...H(av.)	2.0798	-0.0730	2.007(5)	0.1054	2.0920	0.0062	2.098(5)	0.1061	2.098(5)	0.1061
N...Cl(11)	2.9702	-0.0030	2.967(9)	0.0930	2.9733	0.0033	2.977(9)	0.0930	2.974(21)	0.0930
N...Cl(12)	2.8875	-0.0030	2.884(8)	0.0865	2.8944	0.0038	2.898(8)	0.0865	2.894(13)	0.0865
Cl...Cl	3.1326	-0.0024	3.130(7)	0.0963	3.1352	0.0033	3.139(7)	0.0963	3.134(8)	0.0963
C(3)...Cl(11)	3.8259	0.0094	3.835(23)	0.2393	3.8482	0.0512	3.899(23)	0.2417	3.891(48)	0.245(34)
C(3)...Cl(12)	4.1872	-0.0041	4.183(10)	0.1147	4.1786	0.0427	4.221(10)	0.1192	4.222(11)	0.126(10)
C(7)...Cl(11)	3.2936	0.0020	3.296(27)	0.1741	3.3063	0.0214	3.328(33)	0.1757	3.311(66)	0.165(10) ^d
C(7)...Cl(12)	3.3726	-0.0004	3.372(20)	0.1459	3.3591	0.0235	3.383(23)	0.1486	3.384(44)	0.138 ^d
Bond angle										
N—P—Cl(11)			103.0(3)				103.3(3)		103.4(14)	
N—P—Cl(12)			100.5(3)				100.9(3)		100.6(8)	
Cl—P—Cl			97.1(1)				97.2(1)		97.0(2)	
P—N—C(3)			113.8(3)				115.0(4)		115.0(15)	
P—N—C(7)			126.3(4)				125.9(4)		125.7(5)	
C—N—C			111.9(6)				112.6(6)		112.0(10)	
Dihedral angle										
C(3)—N—P—Cl(11)			105.3(14)				107.0(14)		106.5(17)	
C(3)—N—P—Cl(12)			-154.8(15)				-152.8(15)		-153.6(19)	
C(7)—N—P—Cl(11)			-40.9(18)				-42.6(24)		-41.1(36)	
C(7)—N—P—Cl(12)			59.0(19)				57.6(24)		58.8(35)	
Cl(11)—P—N/Cl(12)—P—N (γ)			80.2(1)				79.8(1)		80.2(2)	
C(3)—N—P/C(7)—N—P (δ)			33.8(11)				30.4(14)		32.4(22)	
φ ^e			82.1(13)				82.3(15)		82.7(18)	
R-factor (%)			5.697				5.530		5.456	

Note. The atomic numbering scheme is shown in Fig. 1. The abbreviation av. denotes the average value of the parameter. Listed are the internuclear distances ($r_{ij}/\text{\AA}$), RMS vibrational amplitudes ($u_{ij}/\text{\AA}$), and the estimates of experimental errors including the standard deviation of the least squares method and the scale error²⁹ (in parentheses).

^a Distance between nonbonded atoms.

^{b,c,d} Root-mean-square amplitudes labeled by the same letter were refined in group; in each group, the differences between the amplitudes obtained from spectroscopic calculations were retained.

^e The angle between the bisecting planes of the dihedral angles γ and δ .

cessing errors due to strong correlations. The results obtained with version IIA of structural analysis (r_{h1} -structure) should be considered preferred. In contrast to version I, the use of the r_{h1} -structure allows one to interpret the experimental results in the framework of the harmonic potential approximation, which is most closely related to the equilibrium geometry. This is

confirmed by good agreement between the parameters $r_{ij,h1}$ (they differ from the equilibrium parameters, $r_{ij,e}$, only in the anharmonic contribution) and the results of MP2 calculations of the equilibrium structure (Table 8). If we use the parameters $r_{ij,h0} \equiv r_{ij,e}$, no agreement is observed. Since the estimates $\delta_{ij,anh1}^{\text{vib}}$ for the distances between non-hydrogen atoms are very small (at most

Table 7. Vibrational corrections used for passage from the experimental bond lengths (r_a) in the dimethylaminodichlorophosphine molecule (versions I and IIA of structural analysis, see Table 6) to the parameters r_a^0 and r_{h1}^0 for the ground vibrational state and to the estimates of the parameters of the equilibrium r_e -structure and the values of the parameters of the equilibrium r_e -structure (in Å)

Distance ^a	I ($R = 5.70\%$) ^b		IIA ($R = 5.53\%$) ^b			
	$r_a^0 - r_a$	r_a^0	$r_{h1}^0 - r_a$	r_{h1}^0	$r_e - r_a$	r_e
P—N	−0.0015	1.6684	−0.0002	1.6678	−0.0037	1.6643
N—C(3)	−0.0070	1.4674	0.0010	1.4540	−0.0049	1.4481
N—C(7)	−0.0032	1.4263	0.0007	1.4488	−0.0020	1.4461
C(3)—H(4)	−0.0240	1.0648	0.0017	1.0935	−0.0156	1.0762
C(7)—H(8)	−0.0267	1.0780	0.0017	1.0935	−0.0166	1.0752
C(3)—H(5)	−0.0213	1.0339	0.0016	1.0913	−0.0139	1.0758
C(7)—H(9)	−0.0263	1.0711	0.0017	1.0885	−0.0163	1.0705
C(3)—H(6)	−0.0242	1.0715	0.0016	1.0961	−0.0153	1.0792
C(7)—H(10)	−0.0267	1.0809	0.0016	1.0955	−0.0145	1.0794
P—Cl(11)	−0.0022	2.1110	−0.0008	2.1095	−0.0073	2.1030
P—Cl(12)	−0.0020	2.0704	−0.0007	2.0732	−0.0065	2.0674

^aThe atomic numbering scheme is shown in Fig. 1.

^bSee Table 6.

0.008 Å for $T = 298$ K, see Table 5), the parameters $r_{ij,h1}$ for the distances in the skeleton of molecule **1** can be considered as very good approximation to the equilibrium parameters. It should be noted that the estimates of the parameters $r_{ij,h1}^0$ for chemical bonds (see Table 7) virtually coincide with the parameters $r_{ij,h1}$, whereas the estimates $r_{ij,\alpha} \equiv r_{ij,h0}$ and $r_{ij,\alpha}^0 \equiv r_{ij,h0}^0$ differ appreciably.

Results and Discussion

The estimates of the equilibrium parameters of molecule **1** obtained in this work are substantially different from the recently reported parameters of the r_a -structure³ (see Table 8). This concerns the P—Cl bond lengths (in our opinion, these parameters are underestimated³) and the bond configurations at the P and N

Table 8. Results of experimental structural studies of dimethylaminodichlorophosphine molecule and quantum-chemical calculations of the most stable rotamer **A** (ES) and transition state of inversion at N (**F**, TS_{inv})

Parameter	Experiment			Calculation	
	ED, r_{h1} (325 K) ^a	ED, ³ r_a (295 K)	XRD, ² (143 K) ^b	MP2/6-311G** ² ES	TS_{inv}
<i>r/Å</i>					
P—N	1.668(4)	1.663(4)	1.632(2)	1.669	1.653
N—C(3)	1.454(3)	1.466(8)	1.457(3)	1.467	1.460
N—C(7)	1.449(3)	1.461(8)		1.462	1.458
P—Cl(11)	2.111(5)	2.099(3)	2.093(1)	2.122	2.101
P—Cl(12)	2.074(5)	2.056(3)		2.072	
<i>β/deg</i>					
N—P—Cl(11)	103.3(3)	105.3(11)	103.0(1)	103.7	102.2
N—P—Cl(12)	100.9(3)	101.8(11)		99.9	
Cl—P—Cl	97.2(1)	98.1(5)	94.7(1)	98.7	97.4
P—N—C(3)	115.0(4)	116.2(12)	118.3(2)	114.0	118.6
P—N—C(7)	125.9(4)	126.2(12)	126.6(1)	123.2	126.5
C—N—C	112.6(6)	114.1(17)	114.9(2)	112.5	114.8
<i>τ/deg</i>					
Cl(11)—P—N/Cl(12)—P—N (γ)	79.8(1)	78.0(30)	82.0(2)	78.5	79.4
C(3)—N—P/C(7)—N—P (δ)	30.4(14)	24.7(30)	2.2(2)	31.3	0.0

Note. The atomic numbering scheme is shown in Fig. 1. According to quantum-chemical calculations,² the dipole moments (μ) of ES and TS_{inv} are 3.75 and 4.11 D, respectively, and the relative energy (ΔE) of TS_{inv} is 1.0 kcal mol^{−1}. Notations of experimental methods: XRD denotes X-ray diffraction and ED denotes electron diffraction.

^aThis work.

^bAveraged over two independent molecules in the unit cell.

atoms (earlier,³ they were found to be more "flattened" than in this work). Our conclusion that the amino group has a nonplanar equilibrium configuration is of prime importance. This is a salient feature of the molecular structure of **1** in the gas phase as compared to its structure in the crystal where the amino group is nearly planar.² In addition, the P—N and P—Cl bond lengths change significantly in the crystalline phase. Comparison of the experimental data and the results of quantum-chemical calculations (see Table 8) shows that the gas-phase r_{h1} -structure is in good agreement with the results of MP2/6-311G** calculations of the equilibrium structure (ES), whereas the X-ray diffraction data are in excellent agreement with the parameters obtained from calculations of the TS of inversion at N (TS_{inv}). It is believed that crystal lattice forces are sufficiently strong to compensate the total energy difference between the conformations ES and TS_{inv} even in the absence² of significant van der Waals intermolecular interactions. On the other hand, our calculations of the one-dimensional potential functions and energy levels for the wagging-inversion motion in the amino fragments of the Me₂NNO₂⁴⁵ and Me₂NNO⁴⁶ molecules predict that up to five energy levels can lie below the barrier to inversion (~ 1 kcal mol⁻¹)² in the case of molecule **1**.

Table 9. Comparison of experimental geometric parameters of chloro- and amino-substituted phosphines

Parameter	PCl ₃ , r_g^{29} , $\{r_0\}^{47}$ C_{3v}	Me ₂ NPCl ₂ , gauche- C_1 , r_{h1}^a	(Me ₂ N) ₂ PCl, C_1 , r_a^{48}	P(NMe ₂) ₃ , C_s , r_g^{49}
Bond length				
P—Cl	2.042(2) $\{2.043(3)\}$	2.111(5) 2.074(5)	2.180(4)	—
P—N	—	1.668(4)	1.730(5)	1.703(6) 1.738(6) ^b
Bond angle				
Cl—P—Cl	100.2(2) $\{100.1(4)\}$	97.2(1)	—	—
N—P—Cl	—	103.3(3) 100.9(3)	100.5(7)	—
N—P—N	—	—	96.2(26)	96.8(6) 108.3(6) ^c
C—N—C	—	112.6(6)	120.3(7)	112.5(5) 109.4(5) ^b
P—N—C	—	125.9(4) 115.0(4)	119.8(5)	124.1(5) 116.5(5) 113.6(5) ^b
Sum of angles at P				
300.5	301.4	297.2	301.9	
Sum of angles at N				
—	353.6	359.9	353.1 336.6 ^a	

^aThis work.

^{b,c} Parameters of PNC₂^b or PN₂^c fragments, respectively, for which the local symmetry planes coincide with the molecular symmetry plane.

Gas-phase electron diffraction study¹ of dimethylaminodichlorophosphine first showed that the P—Cl bonds in this molecule are appreciably longer than in PCl₃ (2.04 Å)^{29,47} due to the effect of the amino group. Variations of the geometric parameters of PCl₃, Me₂NPCl₂, (Me₂N)₂PCl, and P(NMe₂)₃ molecules are listed in Table 9. It should be kept in mind that the $r_{ij,h1}$ parameters for bonds, determined in this work, are very close to the experimentally found^{17–20} average parameters $r_{ij,g}$. Changing the type of substituents at the P atom has a pronounced effect on the P—Cl bond length and also affects the P—N bond length. However, these parameters change in the opposite directions, that is, a decrease in the number of Cl atoms leads to lengthening of the P—Cl bonds, whereas the P—N bond in molecule **1** appears to be 0.04 to 0.07 Å shorter than in bis(dimethylamino)chlorophosphine and tris(dimethylamino)phosphine. It should be mentioned that only two P—N bonds in the most stable C_s conformation of the P(NMe₂)₃ molecule have equal lengths. They are 0.03–0.04 Å shorter than the third P—N bond lying in the molecular symmetry plane (the corresponding nitrogen atom is more "pyramidal," *i.e.*, the sum of the bond angles, Σ_N , equals 336.6°, see Table 9). It is noteworthy that the Σ_N values and the bond angles at the N atom in molecule **1** and at the N atoms of the two equivalent P—N bonds in the P(NMe₂)₃ molecule are virtually equal (see Table 9). The sums of the bond angles at phosphorus atoms (Σ_P) in these molecules are virtually independent of the type of substituents.

This work was carried out with the financial support of the Russian Foundation for Basic Research (Project No. 99-03-32511a).

References

1. L. V. Vilkov and L. S. Khaikin, *Dokl. Akad. Nauk SSSR*, 1966, **168**, 810 [*Dokl. Chem.*, 1966 (Engl. Transl.)].
2. N. W. Mitzel, *J. Chem. Soc.*, 1998, 3239.
3. P. E. Baskakova, A. V. Belyakov, A. Haaland, and H. V. Volden, *J. Mol. Struct.*, 2001, **567**–**568**, 203.
4. D. Imberg and H. Friebolin, *Z. Naturforsch. B*, 1968, **23**, 759.
5. A. H. Cowley, M. J. S. Dewar, W. R. Jackson, and W. B. Jennings, *J. Am. Chem. Soc.*, 1970, **92**, 1085.
6. A. H. Cowley, M. J. S. Dewar, W. R. Jackson, and W. B. Jennings, *J. Am. Chem. Soc.*, 1970, **92**, 5206.
7. A. H. Cowley, M. J. S. Dewar, J. W. Gilje, D. W. Goodman, and J. R. Schweiger, *J. Chem. Soc. Chem. Comm.*, 1974, 340.
8. C. Christol and H. Christol, *J. Chem. Phys.*, 1965, **62**, 246.
9. F. Heraud and M. J. Leconte, *C. R. Acad. Sci., Ser. C*, 1966, **262**, 22.
10. J. R. Durig and J. M. Casper, *J. Phys. Chem.*, 1971, **75**, 3837.
11. Sh. Sh. Nabiev and V. D. Klimov, *Zh. Neorg. Khim.*, 1991, **36**, 1254 [*Russ. J. Inorg. Chem.*, 1991, **36** (Engl. Transl.)].
12. S. A. Katsyuba and R. R. Shagidullin, *Zh. Obshch. Khim.*, 1984, **54**, 694 [*J. Gen. Chem. USSR*, 1984, **54** (Engl. Transl.)].

13. A. Rank, J. D. Andose, W. G. Frick, R. Tang, and K. Mislow, *J. Am. Chem. Soc.* 1971, **93**, 6507.
14. A. V. Belyakov, A. Haaland, D. J. Shorokhov, V. I. Sokolov, and O. Swang, *J. Mol. Struct.*, 1998, **445**, 303.
15. S. J. Cyvin, *Molecular Vibrations and Mean Square Amplitudes*, Elsevier, Amsterdam, 1968.
16. K. Kuchitsu and S. J. Cyvin, in *Molecular Structures and Vibrations*, Ed. S. J. Cyvin, Elsevier, Amsterdam, 1972, Ch. 12, 183.
17. V. A. Sipachev, L. S. Khaikin, O. E. Grikina, V. S. Nikitin, and M. Traetteberg, *J. Mol. Struct.*, 2000, **523**, 1.
18. L. S. Khaikin, O. E. Grikina, V. A. Sipachev, A. V. Belyakov, E. T. Bogoradovskii, and M. Kolonits, *J. Mol. Struct.*, 2000, **523**, 23.
19. L. S. Khaikin, O. E. Grikina, V. A. Sipachev, A. A. Granovskii, and V. S. Nikitin, *Izv. Akad. Nauk, Ser. Khim.*, 2000, 616 [*Russ. Chem. Bull., Int. Ed.*, 2000, **49**, 620].
20. L. S. Khaikin, O. E. Grikina, V. A. Sipachev, A. V. Belyakov, and E. T. Bogoradovskii, *Izv. Akad. Nauk, Ser. Khim.*, 2000, 627 [*Russ. Chem. Bull., Int. Ed.*, 2000, **49**, 631].
21. V. A. Sipachev, in *Adv. in Molec. Struct. Res.*, Vol. 5, Eds. I. Hargittai and M. Hargittai, JAI, Greenwich, 1999, 323.
22. V. A. Sipachev, *J. Mol. Struct.*, 1985, 121, *Suppl.: Theochem.*, 1985, **22**, 143.
23. A. B. Burg and P. J. Slota, *J. Am. Chem. Soc.*, 1958, **80**, 1107.
24. A. V. Frost, P. A. Akishin, L. V. Gurvich, G. A. Kurkchi, and A. A. Konstantinov, *Vestn. Mosk. Univ.*, 1953, **12**, 5 (in Russian).
25. L. V. Vilkov, D.Sc. (Chem.) Thesis, M. V. Lomonosov Moscow State University, Moscow, 1968 (in Russian).
26. H. E. Swanson and R. K. Fuyat, *NBS Circular 539*, 1953, Vol. 2, p. 25; STM, Card No. 5-0664.
27. A. W. Ross, M. Fink, and R. H. Hilderbrandt, *International Tables for Crystallography*, International Union of Crystallography, Kluwer, Boston, MA, 1992, Vol. **4**, 245.
28. K. Kuchitsu, M. Nakata, and S. Yamamoto, in *Stereochemical Applications of Gas Phase Electron Diffraction, Part A, Electron Diffraction Technique*, Eds. I. Hargittai and M. Hargittai, VCH, New York, 1988, Ch. 7, p. 227.
29. K. Hedberg and M. Iwasaki, *J. Chem. Phys.*, 1962, **36**, 589.
30. V. A. Sipachev, *J. Mol. Struct.*, 2001, **567—568**, 67.
31. L. S. Bartell, *J. Chem. Phys.*, 1963, **38**, 1827.
32. M. Iwasaki and K. Hedberg, *J. Chem. Phys.*, 1962, **36**, 2961.
33. V. A. Sipachev, *Struct. Chem.*, 2000, **11**, 167.
34. P. Pulay, G. Fogarasi, F. Pang, and J. E. Boggs, *J. Am. Chem. Soc.*, 1979, **101**, 2550.
35. G. Fogarasi and P. Pulay, in *Vibrational Spectra and Structure*, Ed. J. R. Durig, Elsevier, Amsterdam, 1985, Vol. **14**, p. 125.
36. G. Gundersen, S. Samdal, and H. M. Seip, *Least Squares Structural Refinement Program Based on Gas Electron Diffraction Data, Parts I—III*, Department of Chemistry, University of Oslo, Norway, 1980—1981.
37. M. J. Frisch, G. W. Trucks, M. Head-Gordon, P. M. W. Gill, M. W. Wong, J. B. Foresman, B. J. Johnson, H. B. Schlegel, M. A. Robb, E. S. Pople, R. Gomperts, J. L. Anders, K. Raghavachari, J. S. Binkley, C. Gonzales, R. L. Martin, D. J. Fox, D. J. Defrees, J. Baker, J. J. P. Stewart, and J. A. Pople, *GAUSSIAN 92*, Revision C, Gaussian Inc., Pittsburgh (PA), 1992.
38. S. V. Krasnoshchekov, A. V. Abramov, and Yu. N. Panchenko, *Zh. Fiz. Khim.*, 1997, **71**, 497 [*Russ. J. Phys. Chem.*, 1997, **71** (Engl. Transl.)].
39. S. V. Krasnoshchekov, A. V. Abramov, and Yu. N. Panchenko, *Vestn. Mosk. Univ., Ser. 2: Khim.*, 1985, **26**, 29 [*Moscow Univ. Bull., Ser. 2, Chem.*, 1985 (Engl. Transl.)].
40. F. A. Fleming, R. J. Wyma, and R. C. Taylor, *Spectrochim. Acta*, 1965, **21**, 1189.
41. J. R. Durig and J. M. Casper, *J. Cryst. Mol. Struct.*, 1972, **2**, 1.
42. L. S. Khaikin and O. E. Grikina, *17th Austin Symp. on Molecular Structure* (Austin, Texas USA, March 2—4, 1998), Austin, 1998, S11, p. 115.
43. L. S. Khaikin, O. E. Grikina, E. A. Zhilinskaya, and B. I. Zhilinskii, *18th Austin Symp. on Molecular Structure* (Austin, Texas USA, March 6—8, 2000), Austin, 2000, S17, p. 89.
44. L. S. Khaikin, O. E. Grikina, E. A. Zhilinskaya, and B. I. Zhilinskii, *18th Austin Symp. on Molecular Structure* (Austin, Texas USA, March 6—8, 2000), Austin, 2000, S18, p. 90.
45. L. S. Khaikin, O. E. Grikina, V. I. Perevozchikov, A. V. Abramov, V. A. Shlyapochnikov, F. R. Cordell, and J. E. Boggs, *Izv. Akad. Nauk, Ser. Khim.*, 1998, 218 [*Russ. Chem. Bull.*, 1998, **47**, 213 (Engl. Transl.)].
46. L. S. Khaikin, O. E. Grikina, V. I. Perevozchikov, and S. Samdal, *18th Austin Symp. on Molecular Structure* (Austin, Texas USA, March 6—8, 2000), Austin, 2000, S14, p. 86.
47. P. Kisliuk and C. H. Townes, *J. Chem. Phys.*, 1950, **18**, 1109.
48. N. M. Zaripov, V. A. Naumov, and L. L. Tuzova, *Phosphorus*, 1974, **4**, 179.
49. P. E. Baskakova, A. V. Belyakov, Th. Colacot, L. K. Krannich, A. Haaland, H. V. Volden, and O. Swang, *J. Mol. Struct.*, 1998, **445**, 311.

Received January 5, 2001;
in revised form May 7, 2001